Density Functional Theory Studies of $Au_n^+(CH_3OH)_m$ ($n = 3, 5$, $m = 1-5$) Complexes

Ying-Chun Li, Chuan-Lu Yang,* Mei-Yu Sun, Xiao-Xia Li, Yi-Peng An, Mei-Shan Wang, Xiao-Guang Ma, and De-Hua Wang

College of Physics and Electronic Engineering, Ludong University, Yantai 264025, People's Republic of China

Received: September 10, 2008; Revised Manuscript Received: November 10, 2008

The structural, energetic, and electronic properties of gold ions adsorbed methanol, $Au_3^+-(CH_3OH)_m$ ($m = 1-3$) and $Au_5^+-(CH_3OH)_m$ ($m = 1-5$), have been investigated using density functional theory (DFT) within a generalized gradient approximation (GGA). The geometric parameters, vibrational frequencies, adsorption energies, and Mulliken charges are used to analyze the interactions between $Au_{3,5}^+$ clusters and methanol molecules. The present calculations show that more than one methanol molecule can be adsorbed onto small clusters of gold ions and that this adsorption is different from that of single-molecule absorption. The red shift of the C−O stretching frequency decreases as the number of methanol molecules, *m*, increases or as gold cluster size increases. The positive charge on $Au_{3,5}^+$ and coordination number of the adsorption sites on the gold cluster are the dominant factors responsible for the strength of the interactions. We obtained C−O stretching frequencies in $Au_{1,2}^+-(CH_3OH)$ complexes that are below 931 cm^{-1}, which provides theoretical evidence for the experimental observation by Dietrich et al. [*J. Chem. Phys*. **2000**, *112*, 752].

1. Introduction

Gold nanoparticles, by virtue of their potential applications as building blocks for functional nanostructured materials, electronic devices, and nanocatalysts,[1] have been extensively investigated for their reactivity. In addition, because of their nontoxicity and highly biocompatibility they are attractive candidates for therapeutic drug delivery vehicles.[2] Several recent reports have focused on their applications in DNA sequencing and also as microscopy markers.[3] There are several reactions that can occur on nanoparticles, such as catalysis, corrosion, coating, etc., and because these involve adsorption as the first step, adsorption of small molecules onto nanoparticles has been quite thoroughly studied.[4,5] Adsorption of a range of organic molecules including benzene thiol, thiolate,[6] methanol molecules,[7] acetone, diethyl ketone, acetaldehyde,[8] linear molecules of (poly)alkane,[9] planar molecules of thipphene or (poly)pheny thiol/thiolate to gold particles have been studied.[10–14] In addition, a number of experimental and theoretical investigations have been carried out on adsorption of inorganic molecules such as carbon monoxide,[15] hydrogen,[16] and oxygen,[17] among others.

Methanol is a frequent reaction intermediate and a precursor in synthesis, decomposition, and oxidation reactions involving hydrocarbons, such as the Fischer−Tropsch process.[18] For this reason it was chosen as the adsorbate for the gold cluster ion (Au_3^+ and Au_5^+) research reported here. Reactions between methanol and clusters of transition metals such as Fe, Cu, Ag, and Au have previously been observed by infrared photodissociation spectroscopy[19–24] and by Car−Parrinello calculation.[7] In a recent study by Hirabayashi et al. structures of nickel cluster ions adsorbed with methanol, $Ni_3^+-(CH_3OH)_m$ ($m = 1-3$) and $Ni_4^+-(CH_3OH)_m$ ($m = 1-4$), were studied using infrared photodissociation (IR-PD) spectroscopy.[25] The authors also completed the corresponding calculations performed by density functional theory and showed that for the $Ni_3^+-(CH_3OH)_m$ ($m = 1-3$) complexes the length of the Ni−O bond increases and the adsorption energy decreases as *m* increases. In addition, the spectra of the OH stretching vibration for these three complexes have various degrees of red shift beyond that of a free methanol molecule. Thus, the properties of the complexes containing one organic molecule may be different from those containing several, which makes it necessary to investigate multimolecule adsorptions.

In the literature two articles[7,26] about the interactions between methanol molecules and gold cluster ions appear in the same journal volume. One investigated the infrared photodissociation of trapped $Au_n^+-(CH_3OH)_m$ ($n = 1-10$, 15 and $m = 1-3$), focusing on structural and energetic properties of the complexes.[7] The C−O stretching vibration of adsorbed methanol was found to change discontinuously with the red shift decreasing with increasing cluster size *n*. Adducts of up to three CH_3OH molecules on Au_n^+ clusters were investigated, and the red shift also decreased with increasing number of adsorbed methanol molecules. The other paper, performed using Car−Parrinello ab initio molecular dynamics, concerned the structural, dynamical, and electronic properties of $Au_n^+-(CH_3OH)$ and $Au_n-(CH_3OH)$ complexes.[26] The calculation results display similar phenomena regarding the red shift of the C−O stretch frequency in one adsorbed methanol molecule as a function of cluster size *n*, but only the case of one absorbed methanol molecule was considered.

The present work strives to investigate the cases where more than one methanol molecule is adsorbed. Through calculating and analyzing the geometric, energetic, and electronic properties of the $Au_n^+-(CH_3OH)_m$ ($n = 3$, 5, $m = 1-5$) complexes with density function theory (DFT) the present investigations will provide a comprehensive understanding of the interactions between gold clusters and many adsorbed CH_3OH molecules.

2. Computational Approach

All calculations reported in this paper were performed using DFT code DMol3 as implemented in the Material Studio.[27–29] Double numerical quality basis sets with polarization functions (DNP) are used. The DNP basis sets are comparable to 6-31G**

* To whom correspondence should be addressed. Phone: +86-535-6672870. Fax: +86-535-6672870. E-mail: yangchuanlu@263.net.

10.1021/jp808040v CCC: $40.75
Published on Web 01/26/2009

TABLE 1: C−O Stretching Vibration Frequencies in $Au_n^+-(CH_3OH)_m$ Complexes

n	m	ν_{calc}	$\Delta\nu_{calc}$	ν_{exp}
1	1	885.9	147.6	
	2	930.3	103.2	933.0[a]
2	1	913.3	120.2	
	2	952.6	80.9	956.2[a]

[a] The measured peak frequencies, ν_{exp}, are determined by fitting a function to the experimental data. The calculated frequencies are scaled by a factor 0.9786. The values of a free methanol molecule are given for comparison. Reference 7.

sets, and the numerical basis set is much more accurate than a Gaussian basis set of the same size. Here, P refers to inclusion of polarizing functions. For H atoms p functions are included, while for C and O atoms d functions are used. For the Au atom f functions are also included. With the heavy element Au relativistic effects become important in the core electrons and have to be considered in many calculations. One method of incorporating these effects is to use the all electron relativistic option. As the name implies, the core electrons are still included in the calculation, but scalar relativistic effects are added in.[30,31] This is time consuming but can yield more accurate calculation results.

Since the total electrons are odd, spin-unrestricted calculations are used. We applied a gradient-corrected approach using the generalized approximation (GGA) for exchange and correlation in the manner suggested by Perdew−Burke−Ernzerhof (PBE).[32,33] Delley[34] confirmed that the PBE functional with the efficient DNP numerical basis set gives enthalpies of formation for a large set of tested compounds and molecules from the NIST database that are closer to the experimental values than any other method available in DMol3. The estimated error was found to be lower than that obtained with the hybrid B3LYP/6-31G** functional.[34]

The convergence criteria applied during geometry optimization are 1.0×10^{-6} Ha for energy, 4.5×10^{-4} Ha/Å for force, and 0.002 Å for displacement. The self-consistent-field convergence criterion is set so that the root-mean-square (rms) change in the electronic density is less than 1×10^{-5} electrons/Å^3. In all calculations a real orbital cutoff of 5.0 Å is imposed.[29] We performed frequency analysis for each optimized structure to confirm it to be a minimum structure.

3. Results and Discussion

3.1. Red Shift of C−O Stretching Vibration of CH_3OH Adsorbed on Au_3^+ and Au_5^+. In previous experimental work the red shift of a C−O stretching vibration of CH_3OH was found when CH_3OH molecules were adsorbed onto gold ion clusters. However, in some cases no photodissociation was observed within the accessible frequency range. The measured peak frequencies, ν_{exp}, were determined by fitting the experimental data to a Lorentz function. No theoretical work has yet been reported on the frequencies of $Au_n^+-(CH_3OH)_m$ complexes containing several CH_3OH. Therefore, we provide a solution for this problem through our calculations.

To test the reliability of our calculations, we compared the present results of the C−O stretching vibration of adsorbed CH_3OH molecules with those found experimentally. These computational and experimental results are presented in Tables 1, 2, and 3. In a previous experiment, for $n = 1, 2$ and $m = 1$, Dietrich et al.[7] observed no photodissociation within the accessible frequency range and presumed that their respective values were both below 931 cm^{-1}. Our computational values of 885.9 and 913.3 cm^{-1} listed in Table 1 sustain their presumption.

From Tables 1 and 2 we find that when $m = 1$ and $n = 1, 2, 3$, $\Delta v = 147.6$, 120.2, and 99.4 cm^{-1}, respectively, which agrees with experimental results[7] that show the largest red shifts of >100 cm^{-1} are observed when $m = 1$ and $n = 1, 2$. From Tables 2 and 3 we find that our calculation results agree with the experimental values. The frequencies are slightly less red shifted as m increases, which also is in agreement with the experimental results. Through calculation we find that when $n = 3, 5$ for $m = 2$ the frequencies are both about 960 cm^{-1}, which proves that it falls within the range of the Q-branch of CO_2 and is not observed by the experiment. In a word, the calculated C−O stretching vibrations of adsorbed CH_3OH in $Au_n^+-(CH_3OH)_m$ complexes agree well with those measured experimentally. Therefore, it is reasonable to believe that the present calculational level can provide credible calculations for larger $Au_n^+-(CH_3OH)_m$ complexes.

3.2. Structural Properties of $Au_3^+-(CH_3OH)_m$ ($m = 1-3$) Complexes. We first focus on the structural properties of the pure clusters of the gold ion because their energetic, geometrical, and electrical properties will be used in later investigations. Au_3^+ is an equilateral triangle with an Au−Au bond length of 2.60 Å, which is only longer by 0.1 Å than that obtained from ab initio molecular dynamics simulations.[26] For the planar Au_5^+ cluster it has C_{2v} symmetry and consists of three edge-sharing triangles with an average Au−Au bond distance of 2.64 Å, which is in agreement with the value of 2.53 Å reported by Rousseau et al.[26]

In the present calculations the structure optimization of $Au_{3,5}^+-(CH_3OH)_m$ was performed by assuming that the oxygen atom is bound to the on-top site of Au* (asterisk denotes the atom of the adsorption site on the gold cluster). Similar on-top geometries have been suggested for CH_3OH molecules on nickel cluster ions.[25] We attempted to optimize for other adsorption sites, such as bridge and hollow sites; however, the other two geometries also ultimately transform into on-top site geometries. Charged Au_n^+ clusters with one CH_3OH molecule attached have been investigated by Rousseau et al.,[26] who only considered one adsorption site, although different sites with different coordination numbers exist when $n \geq 3$. However, Dietrich et al.[7] investigated the situation where more than one CH_3OH molecule is adsorbed (trapped $Au_n^+-(CH_3OH)_m$, $n = 1-10$, 15 and $m = 1-3$) by infrared photodissociation. Therefore, in the present work we emphasize investigation of the interaction between a Au_n^+ cluster and several CH_3OH molecules or of one CH_3OH molecule adsorbed onto different sites of gold clusters, which results in a series of $Au_3^+-(CH_3OH)_m$ ($m = 1-3$) and $Au_5^+-(CH_3OH)_m$ ($m = 1-5$) complexes.

For a planar Au_3^+ cluster the three vertexes of the equilateral triangle are equivalent, while for the planar Au_5^+cluster its five vertexes can be divided into three types: two two-coordinate (2C) sites (c, e), two three-coordinate (3C) sites (a, b), and one four-coordinate (4C) site (d) (Figure 1.9). Hereafter, letters (a, b, c, d, e) are used to indicate these adsorption sites on a Au_5^+ cluster. Moreover, for the multimolecule adsorption of Au_5^+ clusters there are some equivalent $Au_5^+-(CH_3OH)_m$ complexes. For example, the complex consisting of Au_5^+ and three CH_3OH molecules at (a, c, d) adsorption sites [$Au_5^+-(CH_3OH)_3$ (acd)] has the same configuration as does a $Au_5^+-(CH_3OH)_3$ (bed) complex. Therefore, we studied 22 different $Au_{3,5}^+-(CH_3OH)_m$ complexes in total after excluding equivalent complexes including 3 configurations for the Au_3^+ cluster and 19 for the Au_5^+ cluster.

TABLE 2: Calculated C−O, O−H, Au*−O bond length, Au*−H Distance, Measured and Calculated C−O Stretching Frequencies, and Charges on Au* and O Atoms for $Au_3^+-(CH_3OH)_m$ Complexes

	C−O	O−H	Au*−O	Au*−H	ν_{calc}	ν_{exp}[a]	q_{Au*}	q_O
CH_3OH	1.430	0.971			1033.5	1033.5		−0.486
$Au_3^+-CH_3OH$	1.476	0.976	2.110	2.636	934.1	946	0.222	−0.503
$Au_3^+-(CH_3OH)_2$	1.471	0.975	2.123	2.633	954.3	966.3	0.170	−0.497
	1.473	0.975	2.125	2.630	958.4		0.167	−0.496
$Au_3^+-(CH_3OH)_3$	1.476	0.974	2.140	2.636	961.2	969.1	0.116	−0.494
	1.468	0.974	2.146	2.648	964.1		0.100	−0.489
	1.468	0.974	2.144	2.642	971.8		0.101	−0.492
Au_3-CH_3OH	1.459	0.974	2.190	2.633	976.9		0.056	−0.478
$Au_3-(CH_3OH)_2$	1.458	0.974	2.243	2.621	987.5		−0.039	−0.470
	1.459	0.974	2.237	2.634	971.1		−0.042	−0.471
$Au_3-(CH_3OH)_3$	1.429	0.994	3.305	2.313	1039.6		−0.266	−0.540
	1.466	0.973	2.211	2.649	954.3		−0.015	−0.477
	1.459	0.974	2.238	2.647	984.5		−0.047	−0.471

[a] The measured peak frequencies, ν_{exp}, were determined by fitting a function to the experimental data. The calculated frequencies are scaled by a factor 0.9786. The values of a free methanol molecule are given for comparison. Reference.[7]

Some optimized configurations for the $Au_{3,5}^+-(CH_3OH)_m$ complexes are displayed in Figure 1. The C−O, O−H, Au*−O bond lengths, Au*−H distances, measured and calculated frequencies of C−O stretching mode, and charges on Au* atom and on O atom for the complexes are given in Table 2. In order to study what effects the positive charge has on the structural properties of the complexes the structural parameters of neutral complexes $Au_3-(CH_3OH)_m$ ($m = 1-3$) are also given in Table 2.

For $Au_3^+-(CH_3OH)_m$ ($m = 1-3$) complexes it can be seen from Figure 1.1−1.3 that the bonds between the carbonyl oxygen and the gold atom (Au*−O bond) are all within the plane of the Au_3^+ cluster regardless of whether 1, 2, or 3 methanol molecules are adsorbed onto Au_3^+. From Table 2 we can see that in $Au_3^+-(CH_3OH)_m$ ($m = 1-3$) the length of Au*−O bond increases as m increases. The C−O and O−H bond lengths, which are longer than those found in an isolated CH_3OH molecule, decrease slightly with the increase in m. These changes in the structural parameters are similar to those of $Ni_3^+-(CH_3OH)_m$ ($m = 1-3$).[25] The C−O−H bond angles in the CH_3OH molecule increase from 107.6° to about 109° for the $Au_3^+-(CH_3OH)_m$ ($m = 1-3$) complexes, which is similar to the change of C−C−C bond angles in Au_n−acetone complexes.[8]

We also examine the interaction between the Au atom of the adsorption site and the hydrogen atom. Au*−H (the shortest distance between Au* and the H atom) is about 2.6 Å, while the average Au−Au bond length shortens from 2.59 to 2.57 Å with an increase in m. In contrast to $Au_3^+-(CH_3OH)_m$ complexes the C−O and O−H bonds of $Au_3-(CH_3OH)_m$ complexes are all longer than those of free CH_3OH but shorter than the corresponding bonds of $Au_3^+-(CH_3OH)_m$. Au−O bonds of $Au_3-(CH_3OH)_m$ are longer by about 0.1 Å than the corresponding ones of $Au_3^+-(CH_3OH)_m$. Interestingly, through a large rotation of one adsorbed CH_3OH molecule of the three in $Au_3-(CH_3OH)_3$ one of the hydrogen atoms in the CH_3OH comes closer to Au* with an Au*−H distance 2.313Å. This rotation also makes this CH_3OH molecule remain close to the Au_3 cluster and results in interaction between hydrogen and the Au* atom. However, the Au*−H distances of the other two are 2.649 and 2.647 Å. At the same time, the Au*−O bond length of this adsorption site is 3.305 Å, which is much longer than the others at 2.211 and 2.238 Å, respectively. This phenomenon has not been found in $Au_3^+-(CH_3OH)_3$ complexes. From these results we can conclude that the interactions of Au_3^+ and CH_3OH molecules are stronger than are those of Au_3 and CH_3OH. In a $Au_3^+-(CH_3OH)$ complex the shortest Au−Au bond of the Au_3^+ cluster opposite the adsorption site and the other two adjacent bonds are nearly equivalent, while in $Au_3-(CH_3OH)$ this bond is the longest. In the $Au_3^+-(CH_3OH)_2$ complex the Au−Au bond between two adsorption sites of the Au_3^+ cluster is the longest, while this bond is shortest in $Au_3-(CH_3OH)_2$. These differences in structural parameters of the charged or uncharged complexes should be attributed to the positive charge on Au_3^+.

3.3. Structural Properties of $Au_5^+-(CH_3OH)_m$ ($m = 1-5$) Complexes. The calculation results for three $Au_5-(CH_3OH)$ complexes and $Au_5^+-(CH_3OH)_m$ ($m = 1-5$) complexes are shown in Table 3. For $Au_5^+-(CH_3OH)_m$ ($m = 1-5$) complexes the C−O and O−H bond lengths are longer than those of an isolated CH_3OH molecule and decrease slightly, on the whole, as m increases. All of the C−O−H bond angles increase, but the average Au−Au bond lengths do not show a significant change except in the $Au_5^+-(CH_3OH)_4$ (abce) complex.

In the case where Au_5^+ adsorbs one methanol molecule three different $Au_5^+-(CH_3OH)$ complexes have been studied, and their different adsorption sites are represented as (a), (c), and (d), respectively in Figure 1.4. Corresponding $Au_5-(CH_3OH)$ complexes have also been considered in order to study whether the positive charge affects the structural properties of different adsorption sites to the same extent. The C−O bonds of $Au_5^+-(CH_3OH)$ are all increased beyond that of free CH_3OH, and this is more apparent than for the case of $Au_5-(CH_3OH)$, which is similar to the case of $Au_3^+-(CH_3OH)$ and $Au_3-(CH_3OH)$. The total energy in increasing order is $Au_5^+-(CH_3OH)$(a), $Au_5^+-(CH_3OH)$(c), and $Au_5^+-(CH_3OH)$-(d), while for neutral complexes the order is $Au_5-(CH_3OH)$(c), $Au_5-(CH_3OH)$(a), and $Au_5-(CH_3OH)$(d). Therefore, for these three $Au_5^+-(CH_3OH)$ complexes the extent of the effect of the positive charge is different for the different adsorption sites. We can seen that the most active site on a planar Au_5^+ cluster are site (a, b), not the lowest-coordinate Au atom (c, e).

Six $Au_5^+-(CH_3OH)_2$ complexes are considered with adsorption sites (ab), (ac), (ad) [Figure 1.5], (ce), (ae), and (cd). The difference between the complex with the largest total energy and that with the smallest is 0.27 eV. For $Au_5^+-(CH_3OH)_{1,2}$ complexes the host Au_5^+ has little distortion in $Au_5^+-(CH_3OH)$(d), $Au_5^+-(CH_3OH)_2$(ab), and $Au_5^+-(CH_3OH)_2$(ad); for the others, the Au−O* bonds are all nearly within the plane of the Au_5^+. The O−H bond lengths are all 0.75 Å except those on site (d) of $Au_5^+-(CH_3OH)_2$(ad) and $Au_5^+-(CH_3OH)_2$(cd),

TABLE 3: Calculated C−O, O−H, Au*−O Bond Lengths, Au−H* Distance, Measured and Calculated C−O Stretching Frequencies, and Charges on Au* and O Atoms for $Au_5^+-(CH_3OH)_m$ Complexes

	C−O	O−H	Au*−O	Au−H*	ν_{calc}	ν_{exp}[a]	q_{Au*}	q_O
$Au_5-(CH_3OH)$(a)	1.456	0.973	2.279	2.750	977.4		0.054	−0.465
$Au_5-(CH_3OH)$(c)	1.458	0.974	2.274	2.693	988.0		−0.018	−0.473
$Au_5-(CH_3OH)$(d)	1.451	0.979	2.374	2.637	990.1		0.151	−0.445
$Au_5^+-(CH_3OH)$(a)	1.474	0.976	2.135	2.608	938.3	966.3	0.177	−0.478
$Au_5^+-(CH_3OH)$(c)	1.474	0.976	2.274	2.651	942.5		0.165	−0.497
$Au_5^+-(CH_3OH)$(d)	1.471	0.976	2.176	2.648	944.3		0.200	−0.458
$Au_5^+-(CH_3OH)_2$ (ab)	1.471	0.975	2.171	2.632	953.5	966.3	0.133	−0.491
	1.471	0.975	2.169	2.634	962.0		0.133	−0.491
$Au_5^+-(CH_3OH)_2$ (ce)	1.467	0.975	2.176	2.693	967.4		0.118	−0.493
	1.468	0.975	2.170	2.673	963.0		0.109	−0.490
$Au_5^+-(CH_3OH)_2$ (ae)	1.469	0.975	2.139	2.616	965.1		0.154	−0.479
	1.470	0.975	2.141	2.650	959.0		0.143	−0.494
$Au_5^+-(CH_3OH)_2$ (ad)	1.468	0.975	2.160	2.649	968.7	978.5	0.127	−0.480
	1.467	0.976	2.224	2.644	957.8		0.153	−0.463
$Au_5^+-(CH_3OH)_2$ (ac)	1.470	0.975	2.155	2.637	959.8		0.116	−0.480
	1.467	0.975	2.160	2.680	964.0		0.090	−0.496
$Au_5^+-(CH_3OH)_2$ (cd)	1.470	0.975	2.159	2.651	952.8		0.110	−0.493
	1.469	0.976	2.189	2.623	947.6		0.183	−0.454
$Au_5^+-(CH_3OH)_3$ (abc)	1.464	0.982	2.169	2.616	978.7		0.098	−0.507
	1.476	0.976	2.244	2.679	935.3		0.083	−0.543
	1.467	0.975	2.169	2.662	967.8		0.083	−0.492
$Au_5^+-(CH_3OH)_3$ (ace)	1.466	0.975	2.154	2.625	961.5		0.104	−0.478
	1.463	0.973	2.203	2.707	978.3		0.043	−0.489
	1.466	0.975	2.180	2.673	970.8		0.090	−0.487
$Au_5^+-(CH_3OH)_3$ (acd)	1.463	0.974	2.187	2.684	980.3		0.085	−0.475
	1.465	0.974	2.177	2.681	961.4		0.051	−0.487
	1.463	0.975	2.250	2.696	964.5		0.141	−0.454
$Au_5^+-(CH_3OH)_3$ (bcd)	1.464	0.974	2.171	2.649	981.4		0.101	−0.477
	1.468	0.975	2.170	2.657	959.0		0.103	−0.493
	1.463	0.976	2.249	2.630	971.0		0.137	−0.459
$Au_5^+-(CH_3OH)_3$ (cde)	1.453	0.974	2.333	2.706	992.0		−0.069	−0.470
	1.437	0.982	2.750	2.584	1013.1		0.024	−0.457
	1.454	0.974	2.341	2.713	998.9		−0.126	−0.471
$Au_5^+-(CH_3OH)_3$ (abd)	1.465	0.974	2.187	2.670	964.7		0.116	−0.481
	1.468	0.975	2.218	2.698	966.6		0.130	−0.486
	1.465	0.974	2.219	2.644	971.9		0.112	−0.497
$Au_5^+-(CH_3OH)_4$ (abde)	1.461	0.974	2.212	2.669	973.5		0.077	−0.478
	1.462	0.974	2.250	2.725	977.9		0.059	−0.488
	1.459	0.975	2.299	2.684	972.2		0.119	−0.457
	1.466	0.974	2.187	2.675	958.8		−0.004	−0.489
$Au_5^+-(CH_3OH)_4$ (abce)	1.463	0.974	2.181	2.663	968.4		0.042	−0.487
	1.463	0.974	2.180	2.666	970.1		0.041	−0.486
	1.463	0.974	2.178	2.660	972.6		0.043	−0.488
	1.463	0.974	2.180	2.660	985.1		0.045	−0.487
$Au_5^+-(CH_3OH)_4$ (bcde)	1.464	0.974	2.173	2.642	978.3		0.076	−0.475
	1.465	0.975	2.212	2.679	958.3		0.048	−0.489
	1.460	0.975	2.270	2.621	989.2		0.103	−0.453
	1.459	0.974	2.235	2.719	976.7		−0.034	−0.483
$Au_5^+-(CH_3OH)_4$ (abcde)	1.460	0.975	2.246	2.654	979.1		0.027	−0.483
	1.462	0.974	2.209	2.660	971.3		0.043	−0.481
	1.462	0.974	2.228	2.692	968.4		−0.015	−0.486
	1.454	0.977	2.332	2.602	999.5		0.076	−0.453
	1.458	0.974	2.242	2.706	976.9		−0.066	−0.482

[a] The measured peak frequencies, ν_{exp}, are determined by fitting a function to the experimental data. The calculated frequencies are scaled by a factor 0.9786.[7]

which are 0.76 Å. This can be attributed to the weaker interactions of site (d).

Six stable $Au_5^+-(CH_3OH)_3$ complexes with adsorption sites (abc), (abd) [Figure 1.6], (bcd), (ace), (acd), and (cde) have been found. The structure of $Au_5^+-(CH_3OH)_3$(cde) has the lowest total energy of the six $Au_5^+-(CH_3OH)_3$ complexes, which is lower by 5.1−5.5 eV compared to the other $Au_5^+-(CH_3OH)_3$ complexes. This can be a result of the three C−O bonds of this complex being shorter than the others. For other $Au_5^+-(CH_3OH)_3$ complexes C−O bonds are all more than 1.463 Å, while the longest C−O bond of $Au_5^+-(CH_3OH)_3$(cde) is only 1.454 Å. All of the Au−O bonds of $Au_5^+-(CH_3OH)_3$ complexes lie within the plane of the Au_5^+ cluster except for $Au_5^+-(CH_3OH)_3$(abd). Interestingly, this complex is the one that makes the host Au_5^+ cluster have the most obvious distortion, which is much more obvious than those in $Au_5^+-(CH_3OH)$ (d), $Au_5^+-(CH_3OH)_3$(ab), and $Au_5^+-(CH_3OH)_3$(ad) complexes. In spite of this distortion of geometry the bond lengths of Au_5^+ show no obvious changes when compared with other $Au_5^+-(CH_3OH)_3$ complexes.

For $Au_5^+-(CH_3OH)_4$ complexes $Au_5^+-(C_3H_6O)_4$(bcde), $Au_5^+-(CH_3OH)_4$(abde), and $Au_5^+-(CH_3OH)_4$(abce) [Figure

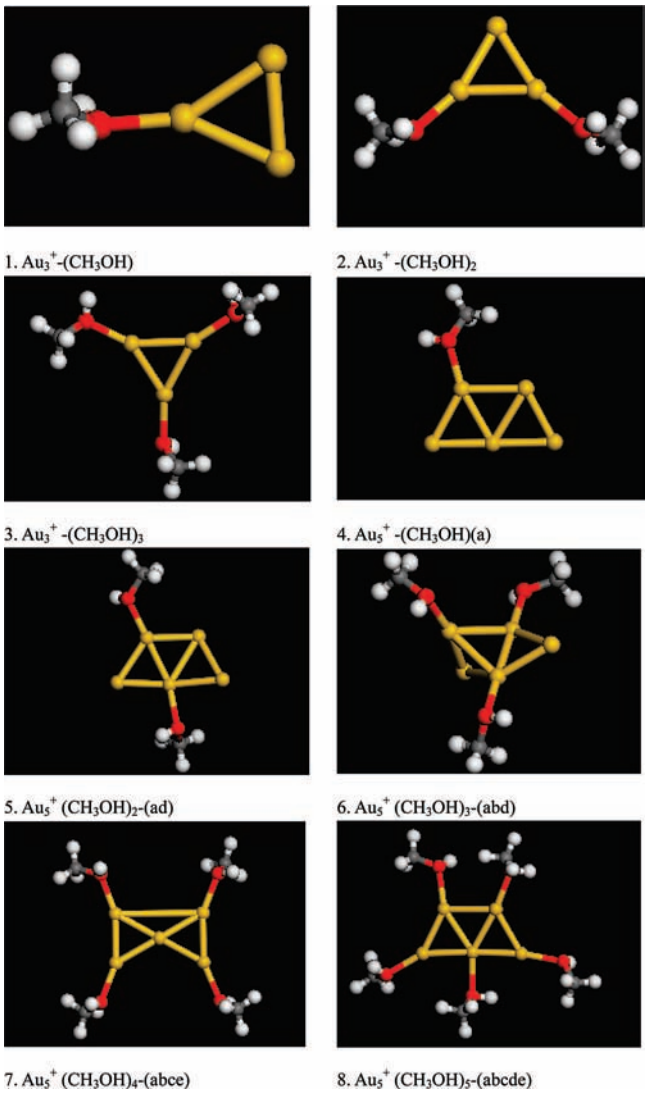

Figure 1. Geometries of $Au_n^+-(CH_3OH)_m$ complexes ($n = 3, 5$, $m = 1-5$). The Au, C, H, and O atoms are shown in yellow, gray, white, and red, respectively.

1.7] have been considered. The total energy of the $Au_5^+-(CH_3OH)_4$ (abce) complex is lower by 0.50 and 0.58 eV than those of the other two complexes. In addition, its interactions change the geometry of the host Au_5^+ cluster, while for the other two $Au_5^+-(CH_3OH)_4$ complexes the geometry of the host Au_5^+ does not display any significant change. Since the case of $Au_5^+-(CH_3OH)_5$(abcde) (Figure 1.8) is similar to that of $Au_5^+-(CH_3OH)_4$ (abde) we will not discuss the former in detail.

3.4. Energetic Properties of $Au_3^+-(CH_3OH)_m$ ($m = 1-3$) and $Au_5^+-(CH_3OH)_m$ ($m = 1-5$) Complexes. To display the characteristics of the energetic interactions among CH_3OH molecules and $Au_{3,5}^+$ we checked the adsorption energies (AEs) of various adsorption cases. The AEs of $Au_3-(CH_3OH)_m$ ($m = 1-3$) and three $Au_5-(CH_3OH)$ complexes have also been considered. The AE between one CH_3OH molecule and the gold cluster can be determined using the expression

$$E_b = E_{Au_n^+-(CH_3OH)} - \left(E_{Au_n^+} + E_{(CH_3OH)}\right) \quad (1)$$

where E_b is the AE between one CH_3OH molecule and the gold cluster, while $E_{Au_n^+}$,$E_{(CH_3OH)}$ are the total energies of the gold cluster ion and the CH_3OH molecule, respectively. We also calculated $E_{b(m)}$ (where m is the number of CH_3OH molecules adsorbed onto the gold cluster), which denotes AE between the mth CH_3OH molecule and the $Au_n^+-(CH_3OH)_{m-1}$ complex because the present investigation systems have several adsorbed molecules. The calculation formula is as follows

$$E_{b(m)} = E_{Au_n^+-(CH_3OH)_m} - \left(E_{Au_n^+(CH_3OH)_{m-1}} + E_{(CH_3OH)}\right) \quad (2)$$

where $E_{Au_n^+-(CH_3OH)_m}$ is the total energy of the $Au_n^+-(CH_3OH)_m$ complex. From Table 4 we can see that the AE between the CH_3OH molecule and the Au_3^+ cluster is 1.69 eV, the second CH_3OH molecule and $Au_3^+-(CH_3OH)$ is 1.49 eV, and the third CH_3OH molecule and $Au_3^+-(CH_3OH)_2$ is 1.27 eV, all of which are much larger than those between Au_3 and CH_3OH, at 0.73, 0.63, and 0.36 eV, respectively. These results clearly show that the interactions of Au_3^+ and the CH_3OH molecule are much stronger than are those of Au_3 and CH_3OH. The AEs seem to decrease when more CH_3OH molecules are adsorbed onto Au_3^+ or Au_3 clusters.

Table 5 displays the AEs of the different adsorption sites for Au_5 and Au_5^+. When one CH_3OH molecule was adsorbed onto Au_5 the order of AE becomes $Au_5-(CH_3OH)$(c) (0.70 eV), $Au_5-(CH_3OH)$(a) (0.62 eV), and $Au_5-(CH_3OH)$(d) (0.45 eV), which is in agreement with the conclusions from coordination number analysis. From these results we can conclude that for neutral Au_5 the energetically preferred adsorption site turns out to be the lowest coordinated site, i.e., the order is site (c) (2C), site (a) (3C), and site (d) (4C). However, for the Au_5^+ cluster the order of the AE changes to become $Au_5^+-(CH_3OH)$(a) (1.46 eV), $Au_5^+-(CH_3OH)$(c) (1.44 eV), and $Au_5^+-(CH_3OH)$(d) (1.25 eV). This significant change in AEs can be attributed to the effect of the positive charge on Au_5^+. Because of the existence of the interactions between Au* and H, Au* and O, and the positive charge the AEs do not

TABLE 4: Adsorption Energies (eV) in $Au_3^+(Au_3)-(CH_3OH)_m$ Complexes

CH_3OH molecule	first	second	third
Au_3^+	1.69	1.49	1.27
Au_3	0.73	0.63	0.36

TABLE 5: Adsorption Energies (eV) of Different Adsorption Sites in a Certain $Au_5^+(Au_5)-(CH_3OH)_m$ Complexes[a]

	a	b	c	d	e
$Au_5-(CH_3OH)$(a)	0.62				
$Au_5-(CH_3OH)$(c)			0.70		
$Au_5-(CH_3OH)$(d)				0.45	
$Au_5^+-(CH_3OH)$(a)	1.46				
$Au_5^+-(CH_3OH)$(c)			1.44		
$Au_5^+-(CH_3OH)$(d)				1.25	
$Au_5^+-(CH_3OH)_2$(ab)	1.21	1.21			
$Au_5^+-(CH_3OH)_2$(ce)			1.09		1.09
$Au_5^+-(CH_3OH)_2$(ae)	1.30				1.29
Au_5^+-$(CH_3OH)_2$(ad)	1.23			1.02	
$Au_5^+-(CH_3OH)_2$(ac)	1.27		1.26		
$Au_5^+-(CH_3OH)_2$(cd)			1.24	1.04	
$Au_5^+-(CH_3OH)_3$(abc)	1.09	1.12	1.16		
$Au_5^+-(CH_3OH)_3$(ace)	1.16		0.96		0.99
$Au_5^+-(CH_3OH)_3$(acd)	0.99		1.00	0.76	
$Au_5^+-(CH_3OH)_3$(bcd)		1.11	1.12	0.85	
$Au_5^+-(CH_3OH)_3$(cde)			6.45	6.40	6.45
$Au_5^+-(CH_3OH)_3$(abd)	1.06	1.06		0.87	
$Au_5^+-(CH_3OH)_4$(abde)	0.82	0.71		0.47	0.77
$Au_5^+-(CH_3OH)_4$(abce)	1.18	1.18	1.05		1.05
$Au_5^+-(CH_3OH)_4$(bcde)		−4.56	0.90	0.68	0.79
$Au_5^+-(CH_3OH)_4$(abcde)	0.69	0.69	0.77	0.19	0.77

[a] The letters a, b, c, d, e denote different adsorption sites.

show an obvious relationship with the corresponding Au*−O bond lengths when one CH_3OH molecule is adsorbed onto different sites. When two CH_3OH molecules are adsorbed at the same time we first consider $Au_5^+-(CH_3OH)_2$(ab) and $Au_5^+-(CH_3OH)_2$(ce), whose two adsorption sites have the same coordination number within a certain $Au_5^+-(CH_3OH)_2$ complex. In these two complexes the AEs of their two adsorption sites are equal (the AEs of sites (a) and (b) are equal to 1.21 eV and those of sites (c) and (e) are equal to 1.09 eV). In addition, the AEs of site (c, e) that has a smaller coordination number are not larger than those of site (a, b) due to the effect of the positive charge. In the other four $Au_5^+-(CH_3OH)_2$ complexes whose two adsorption sites' coordination number are different we can seen that the AEs of two sites within certain complexes take the order of site (a) > site (c) > site(d). For example, in the $Au_5^+-(CH_3OH)_2$ (ac) complex the AE of site (a) (1.27 eV) is larger than that of site (c) (1.26 eV). When three CH_3OH molecules are adsorbed the order of AEs between site (a) and site (c) make an inversion in three of four complexes containing CH_3OH molecules simultaneously at sites (a) and (c). This is because the effect of the positive charge becomes weaker, and the effect of coordination number has been embodied as the number of atoms of the complexes increases. In the case where four CH_3OH molecules are adsorbed the positive charge become mores dispersive and the AEs of different adsorption sites do not display any obvious relationship with either the corresponding Au−O* bond length or the coordination number of the adsorption sites. This is due to the existence of interactions between Au* and H atoms, between Au* and O atoms, and among CH_3OH molecules themselves as well as the effect of the positive charge. In fact, the coordination numbers continue to affect the AEs, but the interactions among CH_3OH molecules themselves become increasingly stronger as the number of CH_3OH molecules increases, which will affect the AE of each site. However, generally speaking, the AE of site (d) in a $Au_5^+-(CH_3OH)_m$ ($m = 2-5$) complex is the smallest among all AEs of the different sites regardless of the number of CH_3OH molecules adsorbed because site (d) is a 4C site that is large enough to counteract the effect of both the interactions among CH_3OH molecules themselves and the positive charge.

It is very interesting that for the $Au_5^+-(CH_3OH)_4$ (abce) complex the geometry of the Au_5^+ host is changed significantly and all AEs become larger than those of the other $Au_5^+-(CH_3OH)_4$ complexes. This can be attributed to the symmetry of the location of the four CH_3OH molecules. For the $Au_5^+-(CH_3OH)_5$ complex the order of the AEs for three different kinds of adsorption sites agree with that seen for Au_5. This may be because the effects of adsorption sites' coordination numbers have become a dominant factor.

3.5. Mulliken Charges of $Au_3^+-(CH_3OH)_m$ ($m = 1-3$) and $Au_5^+-(CH_3OH)$ Complexes. Mulliken charges q (given in units of |e|) for $Au_{3,5}^+$-$(CH_3OH)_m$ and $Au_{3,5}-(CH_3OH)$ complexes are shown in Tables 2, 3, 6, and 7. The charge on the adsorption sites of the gold atom q_{Au*} and the oxygen atom of CH_3OH molecules q_O are presented in Tables 2 and 3. From Table 2 we can see that the positive charge on Au*, q_{Au*}, decreases as m increases for $Au_3^+-(CH_3OH)_m$ ($m = 1-3$) and that the positive charges on Au* are all less than the 0.333|e| of Au_3^+. The negative charge on O, q_O, increases, which is more than −0.486|e| of the free CH_3OH molecule, which decreases slightly with the increase of m. This is due to the negative charge transfer to these two places. For the $Au_5^+-(CH_3OH)$ complex different adsorption sites have different amounts of charge change. For site (a) and site (c) positive charges are 0.214|e| and 0.200|e|, respectively, before adsorption but then become 0.177|e| and 0.165|e|, respectively, which shows that negative charges are arriving at those sites. However, for site (d) the positive charge changes from 0.173|e| to 0.200|e| upon adsorbing one CH_3OH molecule, which means that there is negative charge transfer away from that site. q_{Au*} decreases as m increases for $Au_5^+-(CH_3OH)_m$ ($m = 1-5$) until at $m = 3$ q_{Au*} appears as a negative value.

TABLE 6: Mulliken Charges of $Au_3^+(Au_3)-(CH_3OH)_m$[a]

	$q_{\Delta Au1}$	$q_{\Delta Au2}$	$q_{\Delta Au3}$	$q_{\Delta O}$	$q_{\Delta H}$	$q_{\Delta C}$	$q_{\Delta aveH}$
$Au_3-(CH_3OH)$	0.121	0.124	0.056[b]	0.008	0.053	0.002	0.042
$Au_3^+-(CH_3OH)$	0.072	0.081	0.111[b]	0.017	0.078	0.004	0.067
$Au_3^+-(CH_3OH)_2$	0.164	0.163[b]	0.166[b]	0.011	0.072	0.003	0.061
				0.01	0.072	0.004	0.061
$Au_3^+-(CH_3OH)_3$	0.217[b]	0.233[b]	0.232[b]	0.008	0.067	0.004	0.055
				0.003	0.064	0.003	0.055
				0.006	0.066	0.004	0.055

[a] $q_{\Delta Au}$, $q_{\Delta H}$, and $q_{\Delta aveH}$ denote the absolute value of the amount of charge change for the Au atom, the hydrogen of O−H, and those of average change of each hydrogen atom of CH_3, respectively. [b] Denotes the value of the adsorption site of Au.

TABLE 7: Mulliken Charge of $Au_5^+(Au_5)-(CH_3OH)_m$ Complexes[a]

		a	c	d
Au_5	q_{Au*}	0.007	−0.04	0.065
Au_5^+	q_{Au*}	0.214	0.200	0.173
$Au_5-(CH_3OH)$	$q_{\Delta Au*}$	0.047	0.022	0.086
	$q_{\Delta O}$	0.021	0.013	0.041
$Au_5^+-(CH_3OH)$	$q_{\Delta Au*}$	0.037	0.035	0.027
	$q_{\Delta O}$	0.008	0.028	0.011

[a] q_{Au*} denotes Mulliken charge on the gold atom of Au_5 or Au_5^+ cluster. $q_{\Delta Au*}$ and $q_{\Delta O}$ denote the absolute values of the amount of charge change for adsorption sites on Au_5 or Au_5^+ clusters and oxygen atoms of complexes.

In order to study this transfer of charge more clearly the absolute value for the amount of charge change on some atoms of $Au_3-(CH_3OH)$ and $Au_3^+-(CH_3OH)_m$ ($m = 1-3$) are presented in Table 6. The $q_{\Delta Au}$ on the adsorption site of $Au_3^+-(CH_3OH)$ (0.111) is much larger than that of neutral $Au_3-(CH_3OH)$(0.056). In addition, $q_{\Delta O}$, $q_{\Delta H}$, $q_{\Delta C}$, and $q_{\Delta aveH}$ of $Au_3^+-(CH_3OH)$ are also obviously larger than those of neutral $Au_3-(CH_3OH)$. For this reason, the interactions of CH_3OH molecules and Au_3^+ are stronger than are those between CH_3OH molecules and neutral Au_3. For $Au_3^+-(CH_3OH)_m$ ($m = 1-3$) complexes $q_{\Delta Au}$ increases and $q_{\Delta O}$, $q_{\Delta H}$, and $q_{\Delta aveH}$ decrease as m increases. The degree of change in charge decreases and the interaction becomes weaker as m increases. $q_{\Delta C}$ and $q_{\Delta O}$ are both small, which indicates that charges had little change in these atoms before and after adsorption. In addition, for $Au_3^+-(CH_3OH)_m$ ($m = 1-3$) complexes the positive charge on H atoms of CH_3 increases and on Au* atoms decreases, which can be attributed to the negative charge transferring from hydrogen to gold atoms through oxygen.

The charges on different adsorption sites, q_{Au*}, absolute value of the amount of charge change on adsorption site and O atom, $q_{\Delta Au*}$ and $q_{\Delta O}$, for three different adsorption sites of four structures are shown in Table 7. From this table we can see that the charge distributions on Au_5^+ and Au_5 are different. This can result in a change in the order of AEs of three different adsorption sites. From the order of AEs for Au_5, which is site (c) > site (a) > site (d), and $q_{\Delta Au*}$ on Au_5 we conclude that a lower charge change on a site leads to a larger AE when one CH_3OH molecule is adsorbed on three different sites. For Au_5^+

the order of AE change for sites was site (a) > site (c) > site (d) when one CH_3OH molecule is adsorbed. We also consider q_{Au^*} on Au_5^+ and conclude that a more positive charge of the site leads to a larger AE, and the same conclusion can be drawn for $q_{\Delta Au^*}$. In addition, we find that the AE is not correlated with $q_{\Delta O}$ in either $Au_5^+-(CH_3OH)$ or $Au_5-(CH_3OH)$ complexes.

4. Conclusions

In this paper, we used density functional theory to investigate the adsorption between $Au_{3,5}^+$ clusters and CH_3OH molecules. Our results indicate that more than one CH_3OH molecule can be adsorbed onto $Au_{3,5}^+$clusters. When either Au_3 or Au_3^+ clusters are hosts the AEs decrease as m increases but the interaction between Au_3^+ and CH_3OH is observably stronger than that between Au_3 and CH_3OH. Due to the effect of the positive charge on Au_5^+ clusters the sequence of energetically preferred adsorption sites becomes site (a), site (c), and site (d) when one CH_3OH is adsorbed, which is different from the order site of site (c), site (a), and site (d) of Au_5 clusters. When five CH_3OHs are adsorbed onto Au_5^+ the site order is the same as that for Au_5. It is also found that the positive charge on $Au_{3,5}^+$ clusters, the coordination number of adsorption sites, and the interaction among CH_3OH molecules themselves all affect the AEs. Our calculation results confirm the supposition based on the observation that the C−O stretching frequencies in $Au_{1,2}^+-(CH_3OH)$ complexes are below 931 cm^{-1}. In other words, the cases that include several CH_3OH molecules adsorbed onto gold clusters are notably different from those that include only one CH_3OH molecule. This study has provided a more complete understanding of the interaction between gold clusters and CH_3OH molecules.

Acknowledgment. This work was supported by the National Natural Science Foundation of China under Grant No. 10674114.

References and Notes

(1) Häkkinen, H.; Yoon, B.; Landman, U.; Li, X.; Zhai, H.-J.; Wang, L.-S. *J. Phys. Chem. A* **2003**, *107*, 6168.
(2) West, J. L.; Halas, N. J. *Annu. Rev. Biomed. Eng.* **2003**, *5*, 285.
(3) Jin, R.; Cao, Y.; Mirkin, C. A.; Kelly, K. L.; Schatz, G. C.; Zheng, J. G. *Science* **2001**, *294*, 1901.
(4) Somorjai, G. A. *Introduction to Surface Science and Catalysis*; Wiley: New York, 1994.
(5) Newns, D. M.; Muscat, J. P. *Prog. Surf. Sci.* **1978**, *9*, 1.
(6) Letardi, S.; Cleri, F. *J. Chem. Phys.* **2004**, *120*, 10062.
(7) Dietrich, G.; Krückeberg, S.; Lützenkirchen, K.; Schweikhard, L.; Walther, C. *J. Chem. Phys.* **2000**, *112*, 752.
(8) Shafai, G. S.; Shetty, S.; Krishnamurty, S.; Shah, V.; Kanhere, D. G. *J. Chem. Phys.* **2007**, *126*, 014704.
(9) Lavrich, D. J.; Wetterer, S. M.; Bernasek, S. L.; Scoles, G. *J. Phys. Chem. B* **1998**, *102*, 3456.
(10) Riederer, D. E.; Chatterjee, R.; Rosencrance, S. W.; Postawa, Z.; Dunbar, T. D.; Allara, D. L.; Winograd, N. *J. Am. Chem. Soc.* **1997**, *119*, 8089.
(11) Joo, S. W.; Han, S. W.; Kim, K. *J. Colloid Interface Sci.* **2001**, *240*, 391.
(12) Gottschalck, J.; Hammer, B. *J. Chem. Phys.* **2002**, *116*, 784.
(13) Majumder, C.; Briere, T. M.; Mizuseki, H.; Kawazoe, Y. *J. Chem. Phys.* **2002**, *117*, 2819.
(14) McNally, H.; Janes, D. B.; Kasibhatla, B.; Kubiak, C. P. *Superlattices Microstruct.* **2002**, *31*, 239.
(15) Zhai, H.-J.; Wang, L.-S. *J. Chem. Phys.* **2005**, *122*, 051101.
(16) Varganov, S. A.; Olson, R. M.; Gordon, M. S.; Metiu, H. *J. Chem. Phys.* **2004**, *120*, 5169.
(17) Varganov, S. A.; Olson, R. M.; Gordon, M. S.; Mills, G.; Metiu, H. *J. Chem. Phys.* **2003**, *119*, 2531.
(18) Ichihashi, M.; Hanmura, T.; Yadav, R. T.; Kondow, T. *J. Phys. Chem. A* **2000**, *104*, 11885.
(19) Zakin, M. R.; Brickman, R. O.; Cox, D. M.; Reichmann, K. C.; Trevor, D. J.; Kaldor, A. *J. Chem. Phys.* **1986**, *85*, 1198.
(20) Knickelbein, M. B. *Chem. Phys. Lett.* **1995**, *239*, 11.
(21) Knickelbein, M. B. *J. Chem. Phys.* **1996**, *104*, 3517.
(22) Dietrich, G.; Dasgupta, K.; Krückeberg, S.; Lützenkirchen, K.; Schweikhard, L.; Walther, C.; Ziegler, J. *Chem. Phys. Lett.* **1996**, *259*, 397.
(23) Knickelbein, M. B.; Koretsky, G. M. *J. Phys. Chem. A* **1998**, *102*, 580.
(24) Rousseau, R.; Dietrich, G.; Krückeberg, S.; Lützenkirchen, K.; Marx, D.; Schweikhard, L.; Walther, C. *Chem. Phys. Lett.* **1998**, *295*, 41.
(25) Hirabayashi, S.; Okawa, R.; Ichihashi, M.; Kondow, T.; Kawazoe, Y. *J. Phys. Chem. A* **2007**, *111*, 7664.
(26) Rousseau, R.; Marx, D. *J. Chem. Phys.* **2000**, *112*, 761.
(27) Delley, B. *J. Chem. Phys.* **1990**, *92*, 508.
(28) Delley, B. *J. Chem. Phys.* **2000**, *113*, 7756.
(29) *Accelrys, Materials Studio*, Release 4.0; Accelrys Software, Inc.: San Diego, 2006.
(30) Koelling, D. D.; Harmon, B. N. *J. Phys. C: Solid State Phys.* **1977**, *10*, 3107.
(31) Douglas, M.; Kroll, N. M. *Acta Phys.* **1974**, *82*, 89.
(32) Perdew, J. P.; Burke, K.; Ernzerhof, M. *Phys. Rev. Lett.* **1996**, *77*, 3865.
(33) Perdew, J. P.; Burke, K.; Ernzerhof, M. *Phys. Rev. Lett.* **1997**, *78*, 1396(E).
(34) Delley, B. *J. Phys. Chem. A* **2006**, *110*, 13632.

JP808040V